Overview of Alcator C-Mod Research Program

S. Scott for the C-Mod team

21st IAEA Fusion Energy Conference

Chengdu, China

16-21 October, 2006

PaperOV/3-2

Work supported by US DoE Office of Fusion Energy Sciences

Explore a range of physics issues of interest to ITER in ITER-like regimes

Alcator C-Mod

- Magnetic field
- Plasma density and pressure
- Equilibrated ions / electrons
- High-Z PFCs
- Power density in SOL
- Divertor opacity to neutrals and radiation
- Momentum input and fueling decoupled from heating and current drive

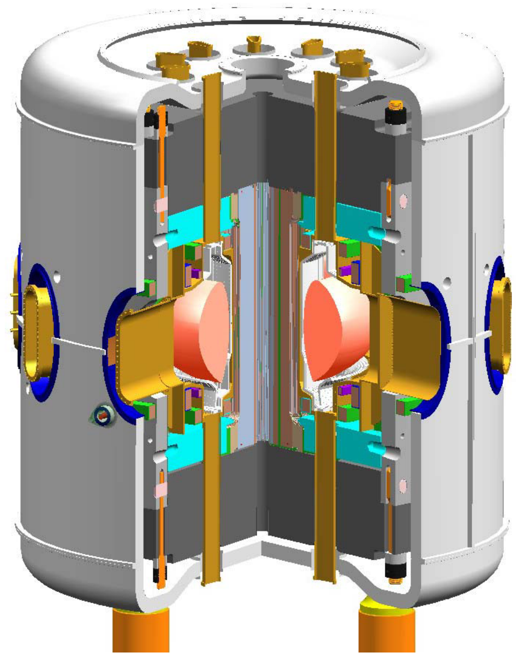

Topics

- Peformance with all-metal walls and physics of 'boronization'
- Initial results with Lower Hybrid Current Drive
- MHD studies: disruption mitigation, locked modes
- Alfven Cascades
- Turbulence measurements & simulations (TEM)
- Scaling of 'intrinsic' toroidal rotation
- The plasma edge: SOL transport, 'blob' dynamics, ELMs

Extensive Campaign to Characterize Performance with All-metal walls and Effect of Boronization

Alcator C-Mod

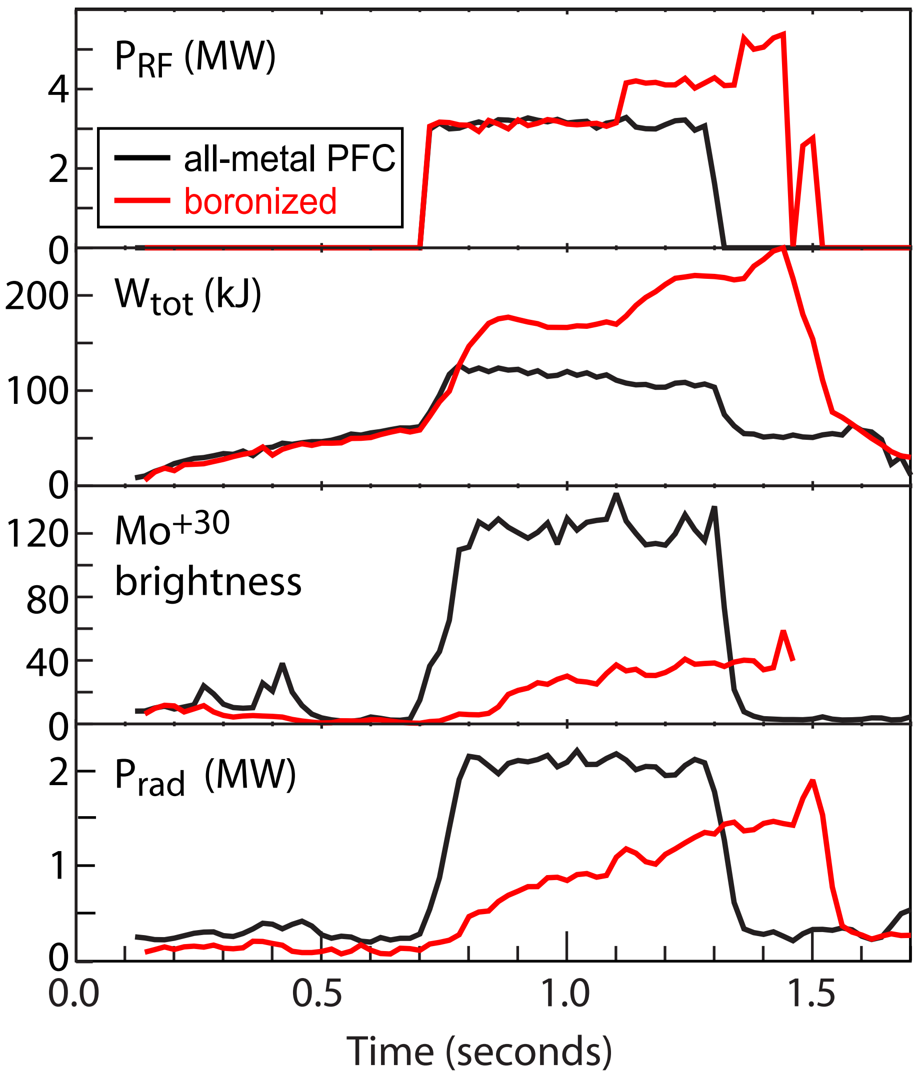

Motivation:

- ITER τ_E projections are based mostly on confinement expts with low-Z PFCs or low-Z wall coatings (Li, Be, B).
- W chosen for ITER based on hydrogen retention, neutron damage, etc. despite low allowable concentration ($\sim 10^{-4}$).

C-Mod (< 2005) Mo walls, overnight boronization since 1996; BN tiles in 2000

CY 2005-06 campaign

- Removed boron from PFCs (~10% left).
- Removed BN tiles
- Extended campaign with all-metal PFCs.
- Then compare to overnight or between-shot boronization.

Result: consistently higher performance with boron: Lower P_{rad}, lower n_{Mo}, higher $W_{tot.}$ Record tokamak $\langle p \rangle$ = 1.8 atm at β_n = 1.74.

Marmar, EX/3-4

Performance with all-metal (Mo) PFCs is limited by radiation from molybdenum impurity

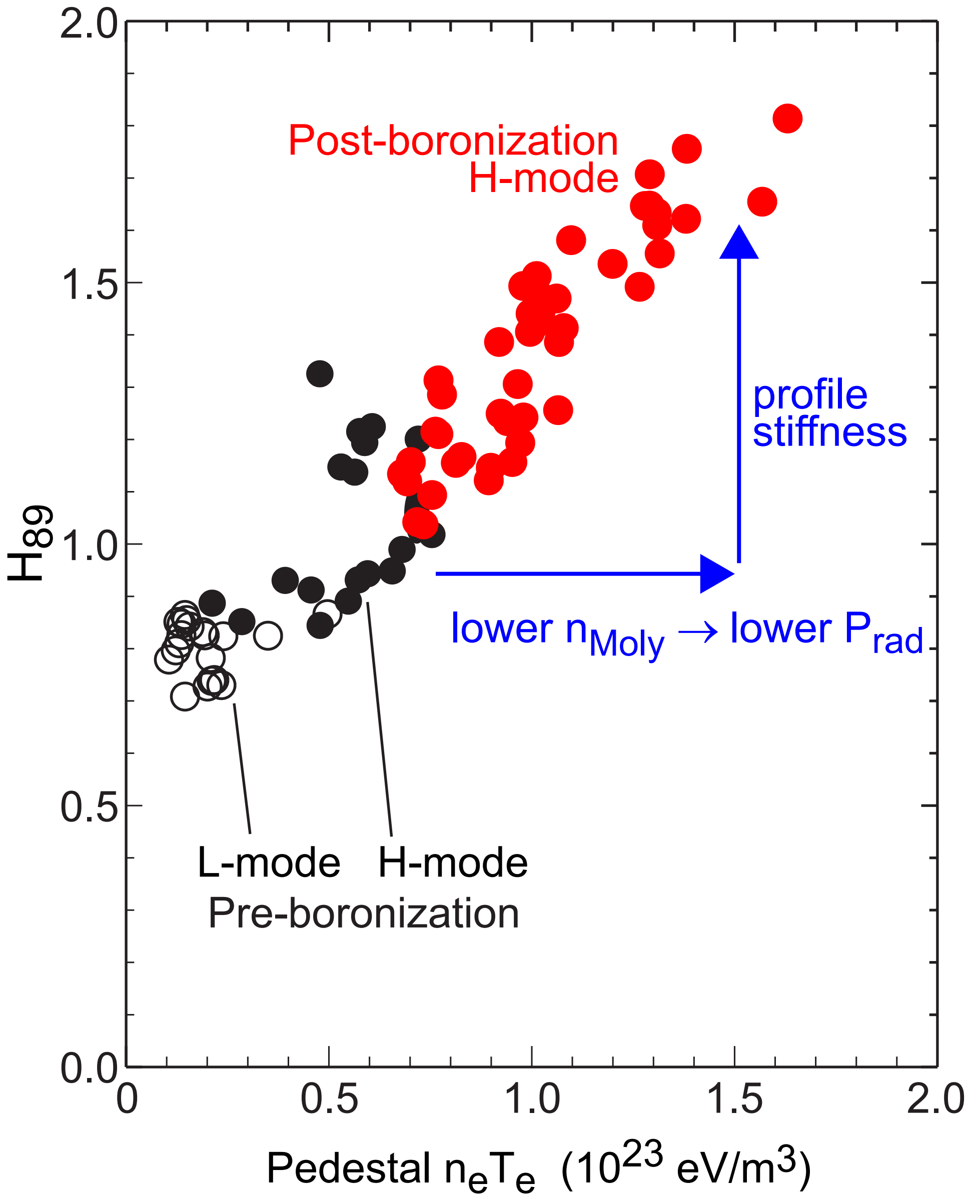

- H-modes readily achieved with all-metal PFCs, but P_{rad} is high and $H_{89p} < 1.3$.
- Overnight boronization (200 nm) reduces $n_{Mo} > 5$x.
- Lower n_{Mo} reduces $P_{rad} \Rightarrow$ increases power flow through SOL $\Rightarrow$ pedestal pressure increases.
- Profile 'stiffness' propagates increased P_{ped} to improved global τ_E.
- Favorable effects wear off in 20-50 shots, or ~50 MJ deposited RF energy.
- Enhanced sheath potential by ICRF at specific locations is identified as cause of boron erosion and impurity generation.

Marmar, EX/3-4, Wukitch, FT/1-6

Significant D retention is observed with all-metal PFCs

Retention a function of plasma density but not plasma regime

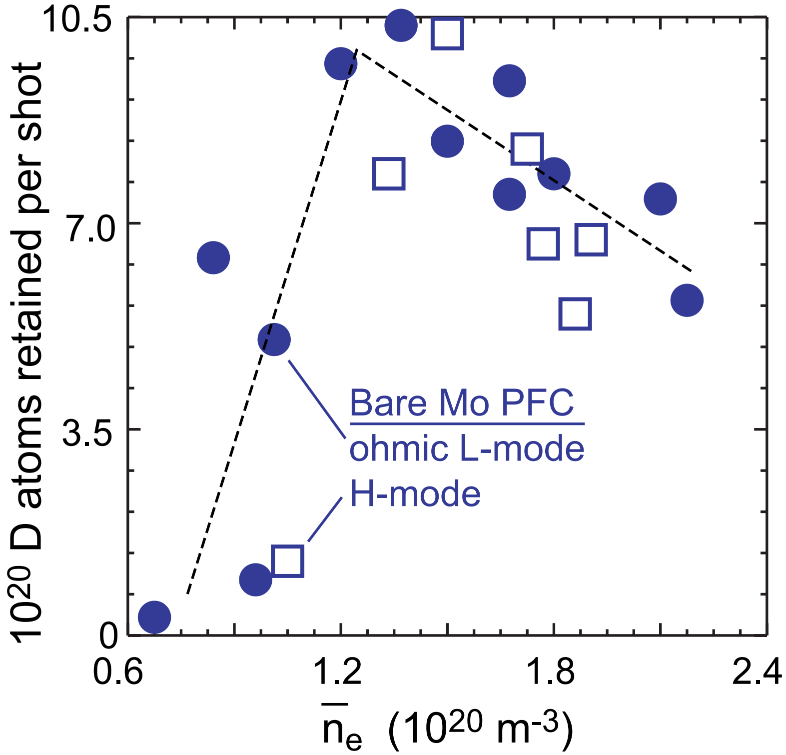

Significant D retention is observed with all-metal PFCs

Alcator C-Mod

Retention in C-mod is not caused by co-deposition with boron

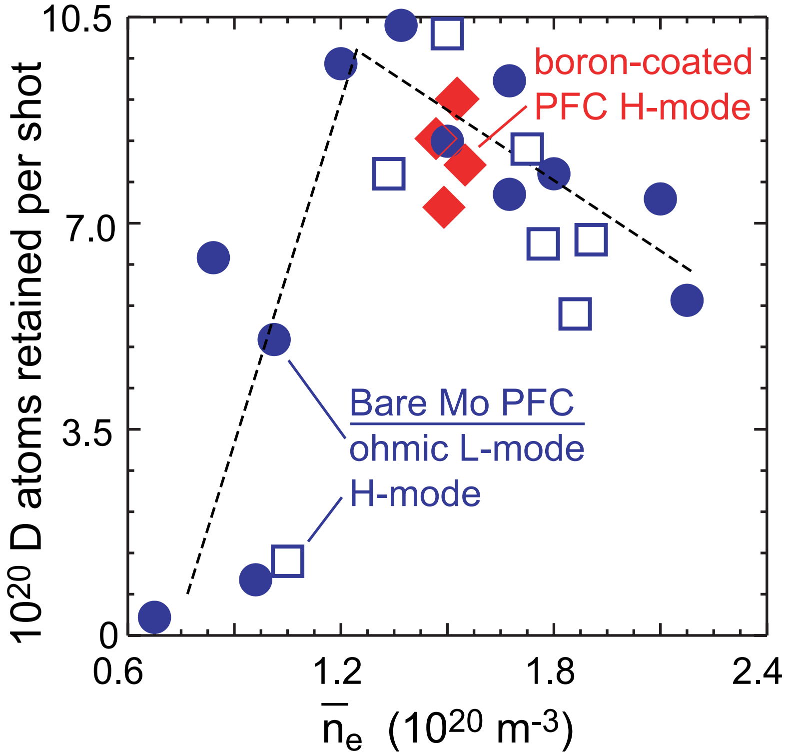

No evidence of saturation in consecutive, non-disruptive shots

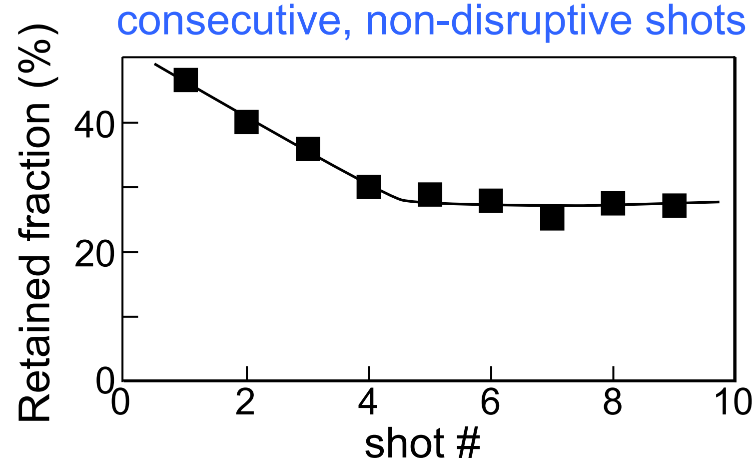

Retention inconsistent with models based on ion beam data

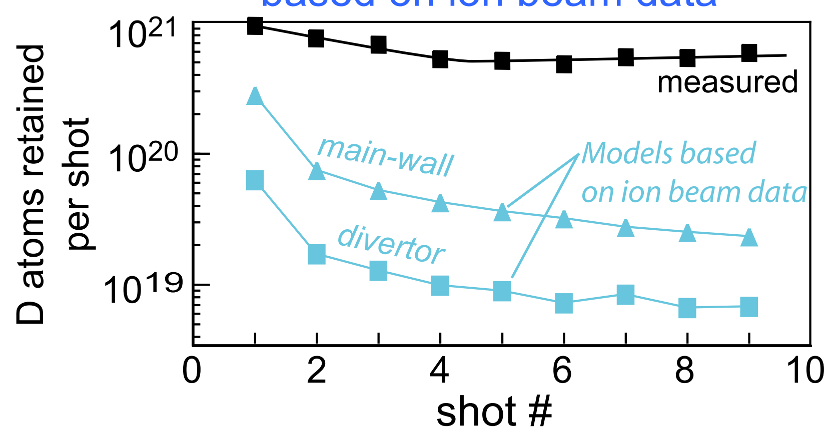

- Similar retention rates observed with all-metal versus boronized PFCs: 20-40% of fuelled gas, ~0.5% of incident ion flux.

- DIONISOS facility will expose Mo target to high-flux, low-energy D plasma to study retention & saturation.

Whyte, EX/P4-29

Major goal of C-Mod program is to study LHCD and its application to high performance integrated AT Plasmas

Alcator C-Mod

Objective: inform decision on LHCD for ITER & enhance prospects for ITER's hybrid and steady-state operations.

- measure LH coupling, current-drive efficiency, control of j(r).
- benchmark LH codes (GENRAY/CQL3D) used to model proposed AT regimes for ITER.
- LH wave physics similar on C-Mod and ITER (ω_{pe}, ω_{ce}).

LHCD system: 3.0 MW (source)
$n_{||}$ = 1.5 - 4.5, 4 x 24 grill

Accome modeling of LHCD indicates fully steady-state, high-performance regimes are accessible

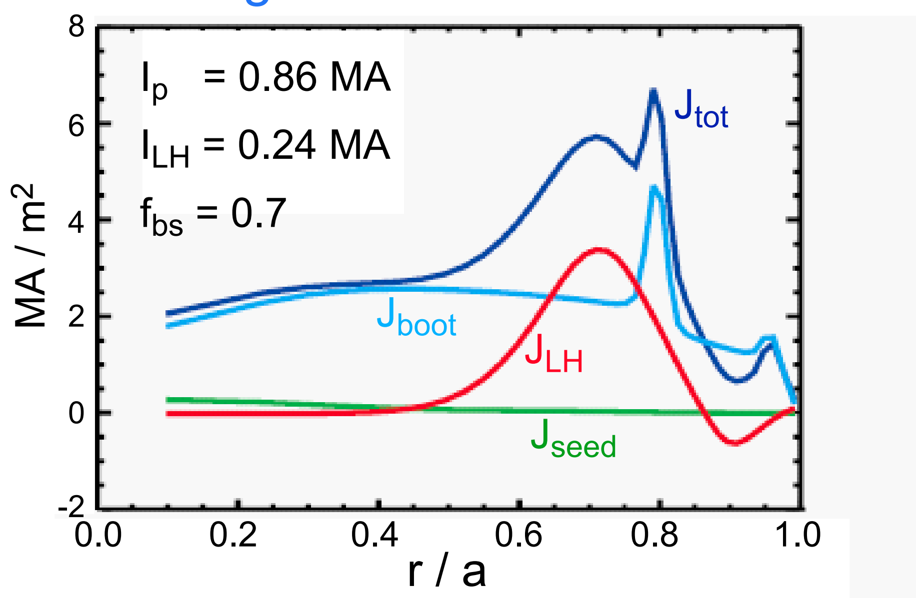

Initial LHCD results are promising: V_{loop} ~0 V at I_p = 1.0 MA for ~200 ms at I_p = 1.0 MA

Alcator C-Mod

P_{LH} = 800 kW, 60° phasing, $n_{||}$ = 1.6, $\tau_{CR} \approx$100 ms

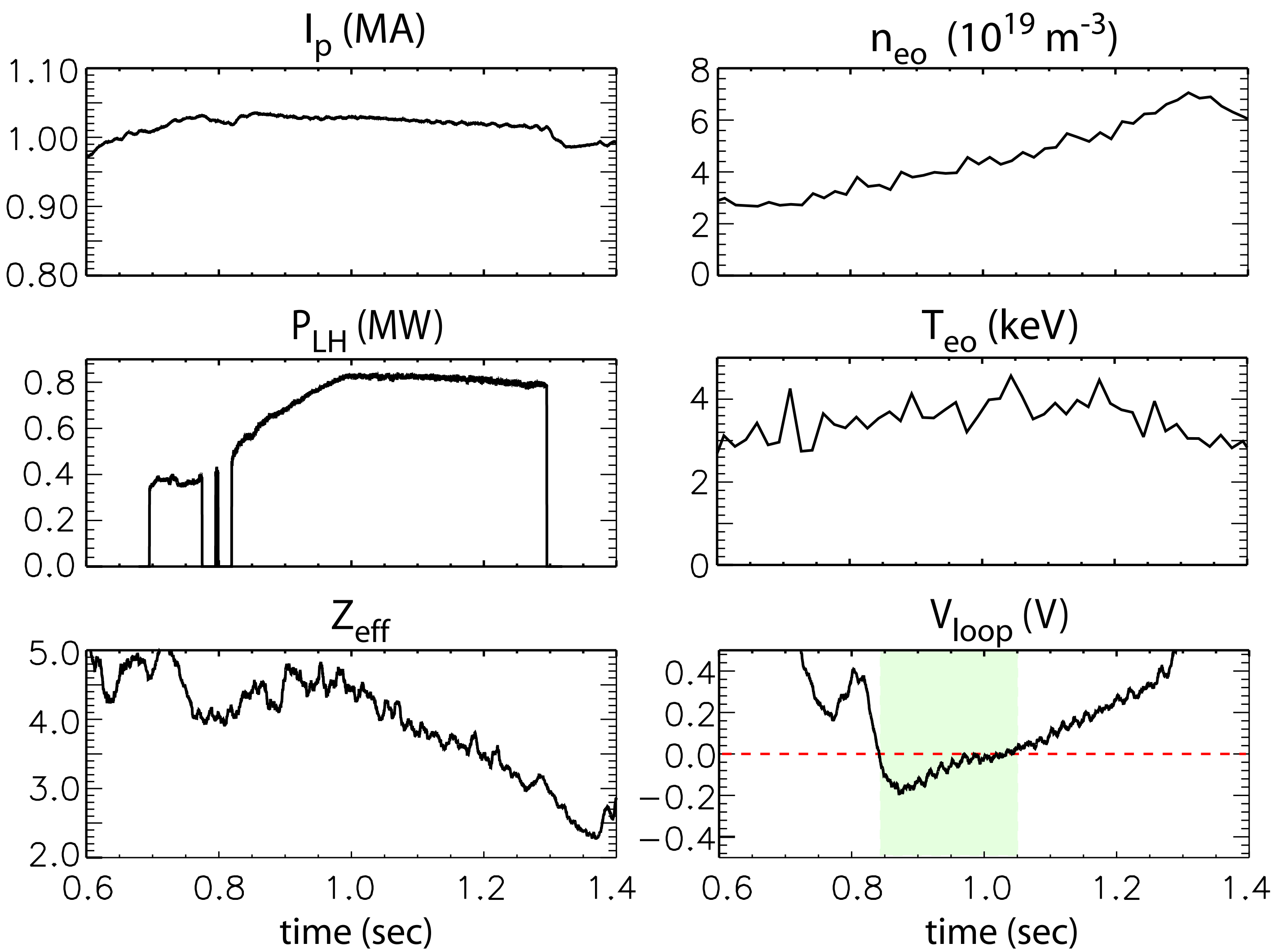

- Reflection coefficients agree with Brambilla code assuming ~ 1 mm vacuum gap.
- No evidence of anomalous impurity influx.
- Sawteeth stabilized.
- Measurements of x-ray spectra and emissivity profile agree qualitatively with expectations.

LH current drive efficiency determined from power scaling is favorable

Loop voltage reduction versus normalized P_{LH}

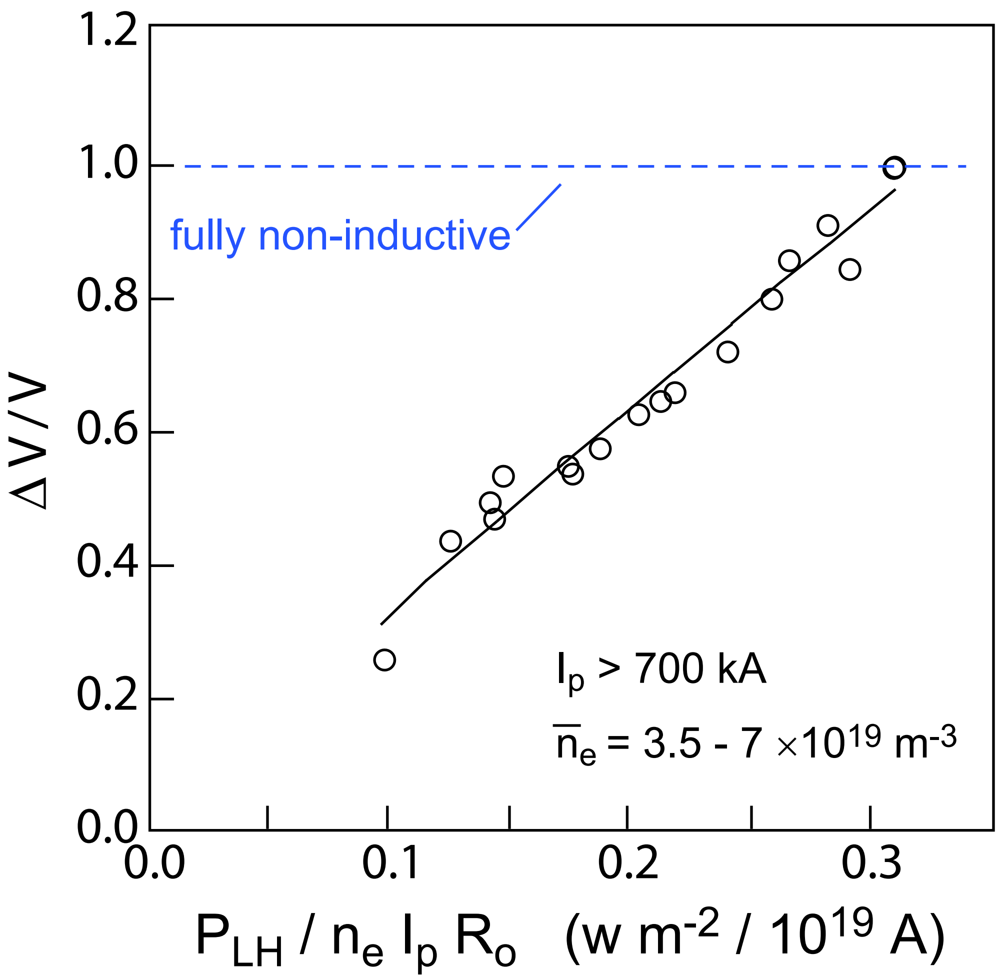

- All shots with 60° phasing, $n_{||} = 1.6$.
- $P_{LH} = 120 - 830$ kW.
- Efficiency: $\overline{n}_{20}\, IR/P_{LH} \approx 0.26$
- Efficiency consistent with Genray-CQL3D modelling and ~30% above Accome.

  $\Rightarrow$ promising for future AT studies.

Disruption mitigation via gas jet injection shows promise for ITER even at high plasma pressure

- Technique (DIII-D): inject massive amount impurity gas to radiate W_{tot} isotropically during disruption. P_{rad} ~1 GW needed in C-Mod.
- Extend mitigation to ITER-like plasma pressure (these expts ⟨p⟩ = 0.8 atm, ITER = 1.75).

Radiated energy fraction increases with Z_{gas}, reaching ~80-90%

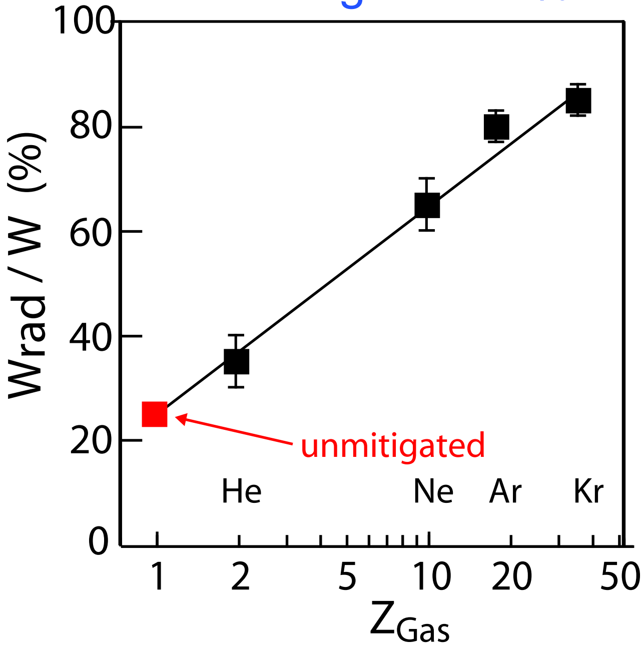

Halo currents reduced ~50%

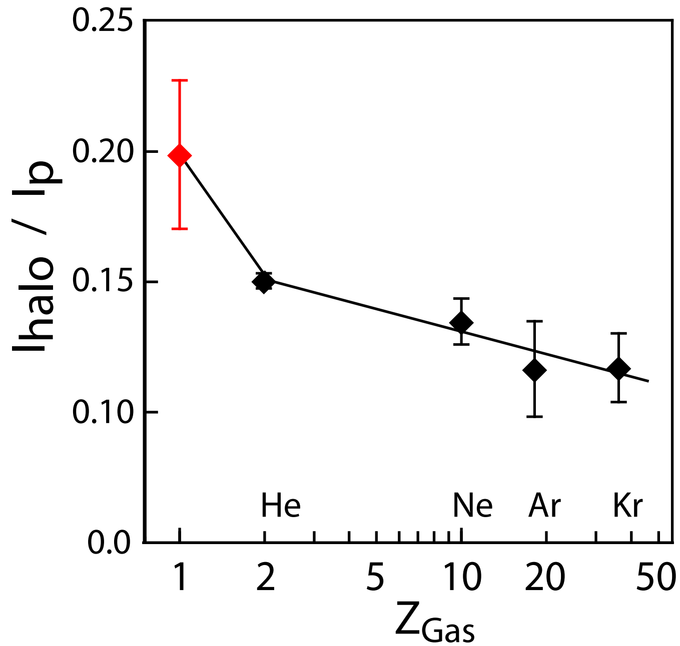

Divertor tile heating reduced ~60%

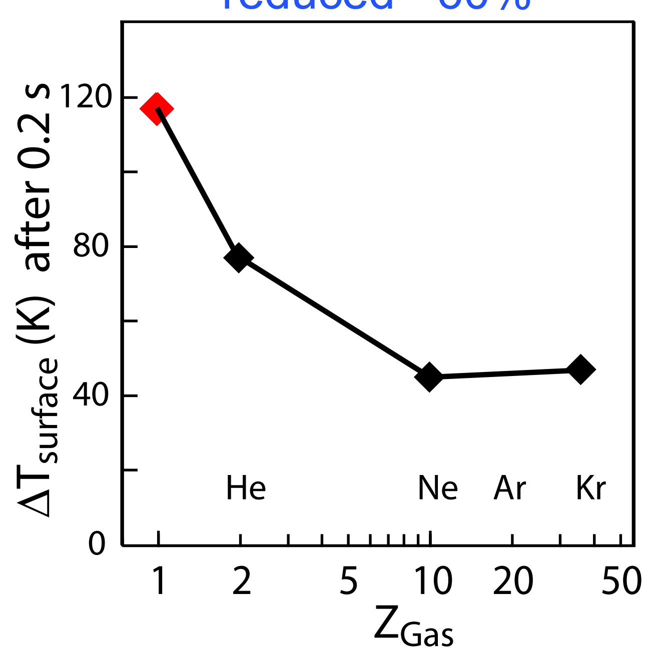

- Gas mixture (90% He, 10% Ar) obtains favorable radiative properties of high-Z with rapid transit of helium through gas delivery system.

Granetz, EX/4-3

NIMROD MHD simulations show edge cooling triggers 1/1, 2/1 tearing modes, leading to stochasticity

- In both DIII-D and C-Mod, high-speed imaging of gas jet plumes shows that impurity neutrals do not penetrate past plasma edge.
- Nevertheless, energy throughout plasma is radiated in 1-2 ms. How?
- NIMROD: growth of 1/1, 2/1 $\Rightarrow$ stochastic field lines $\Rightarrow$ core energy transported to edge $\Rightarrow$ radiated by impurities.
- Favorable for ITER: direct penetration of neutral gas is not necessary.

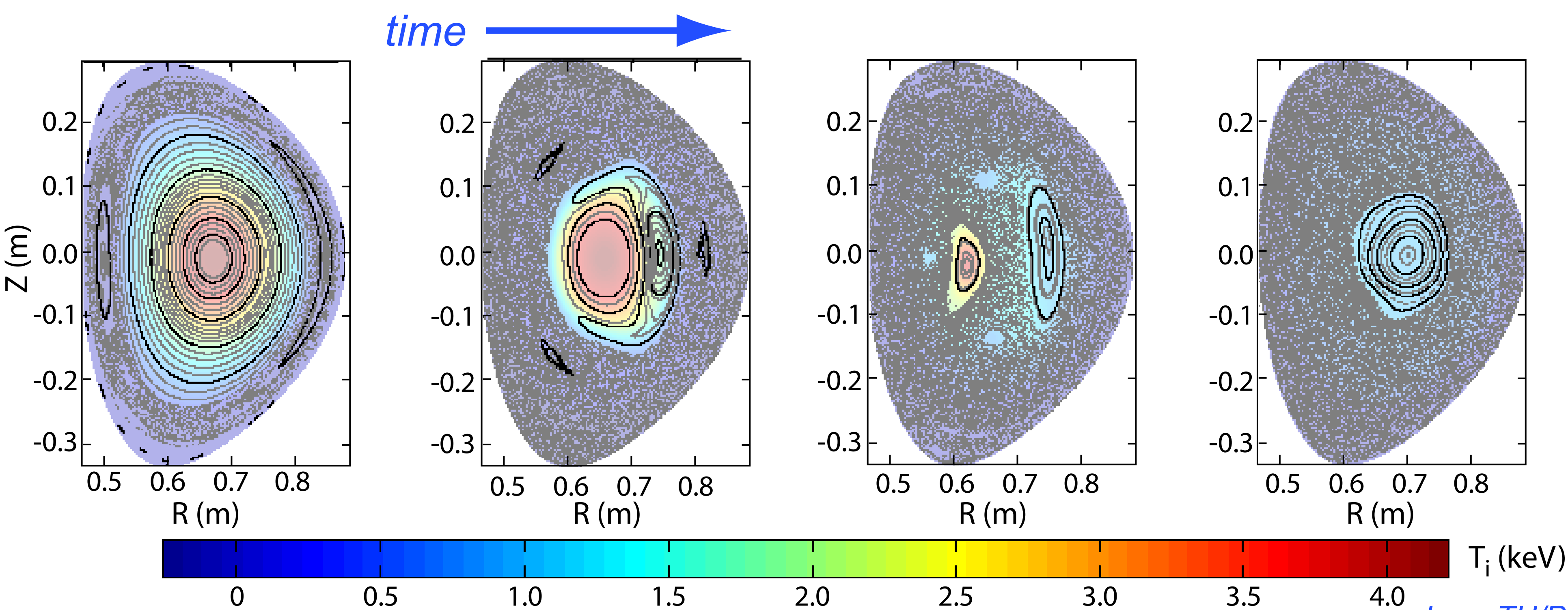

Izzo, TH/P3-15

B_T Scaling of Error Field for Locked Modes Implies a Radius Scaling Favorable for ITER

Parameterization of locking threshold:

$$\frac{\tilde{B}}{B_T} \propto n^{\alpha_n} B^{\alpha_B} q^{\alpha_q} R^{\alpha_R}$$

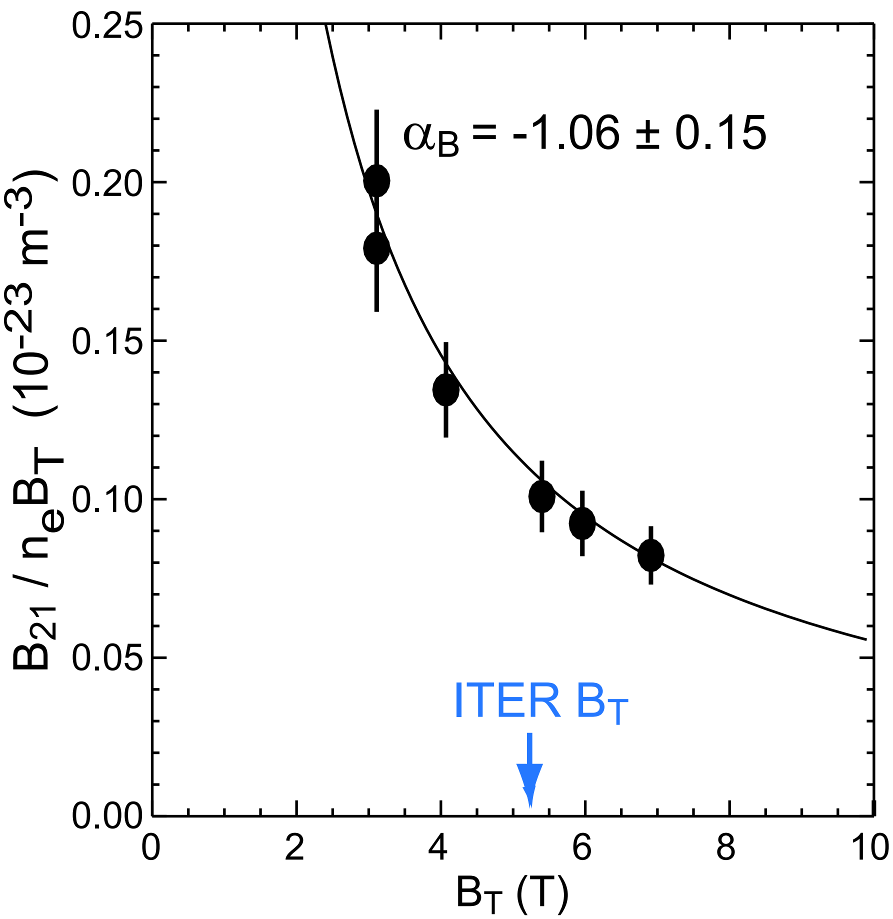

- Scaling of $\tilde{B}$ / B_T locking threshold is needed to extrapolate to ITER.

  α_n = 1 (experiment)

  $\alpha_R = 2\alpha_n + 1.25\,\alpha_B$ (Connor-Taylor)

- C-Mod expt: B_T scan with $n \propto I_p \propto B_T$, $n/n_G = 0.17$, q_{95} =3.5, $\tilde{B}_{11}/\tilde{B}_{21} = 1.4$.

- C-Mod data implies $\alpha_R = 0.68 \pm 0.19$ and projects to $\tilde{B}_{21}/B = 0.9 \times 10^{-4}$ at ITER's ohmic density (within ITER design constraint).

B_T Scaling of Error Field for Locked Modes Implies a Radius Scaling Favorable for ITER

Parameterization of locking threshold:

$$\frac{\tilde{B}}{B_T} \propto n^{\alpha_n} B^{\alpha_B} q^{\alpha_q} R^{\alpha_R}$$

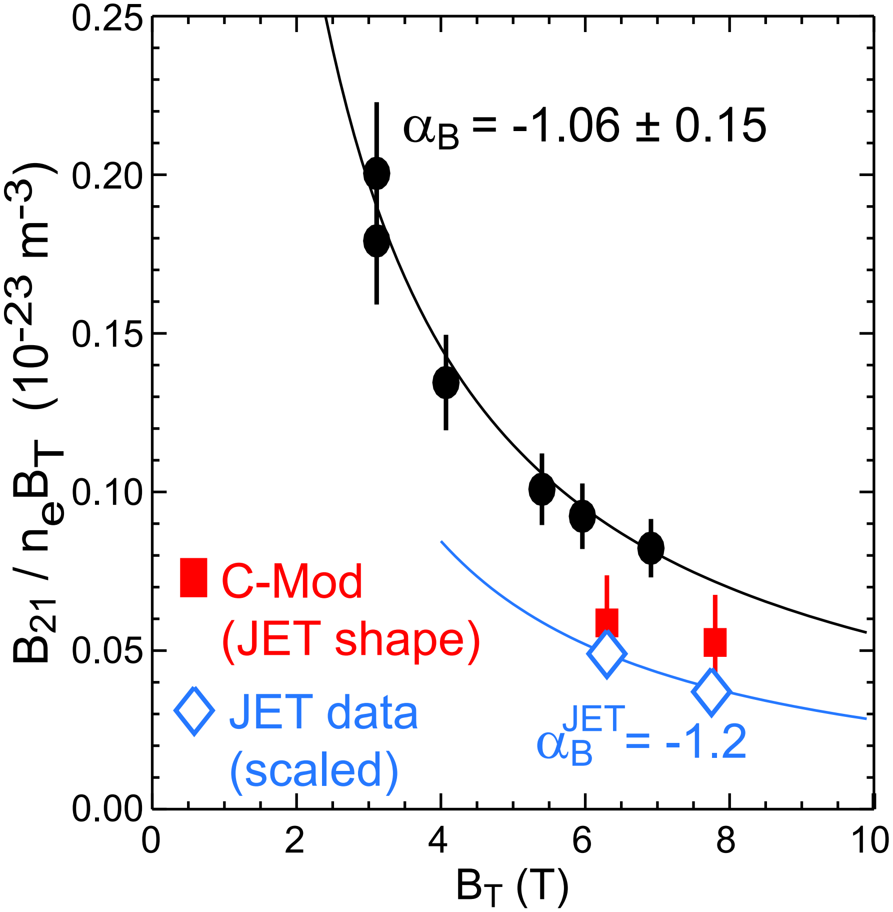

- Scaling of $\tilde{B} / B_T$ locking threshold is needed to extrapolate to ITER.

  $\alpha_n = 1$ (experiment)

  $\alpha_R = 2\alpha_n + 1.25\,\alpha_B$ (Connor-Taylor)

- C-Mod expt: B_T scan with $n \propto I_p \propto B_T$, $n/n_G = 0.17$, $q_{95} = 3.5$, $\tilde{B}_{11} / \tilde{B}_{21} = 1.4$.

- C-Mod data implies $\alpha_R = 0.68 \pm 0.19$ and projects to $\tilde{B}_{21}/B = 0.9 \times 10^{-4}$ at ITER's ohmic density (within ITER design constraint).

- JET/C-Mod identity experiments: JET shape, $\tilde{B}_{11} / \tilde{B}_{21} = 2.1$. Confirms Connor-Taylor & $\alpha_n = 1$.

B_T Scaling of Error Field for Locked Modes Implies a Radius Scaling Favorable for ITER

Parameterization of locking threshold:

$$\frac{\tilde{B}}{B_T} \propto n^{\alpha_n} B^{\alpha_B} q^{\alpha_q} R^{\alpha_R}$$

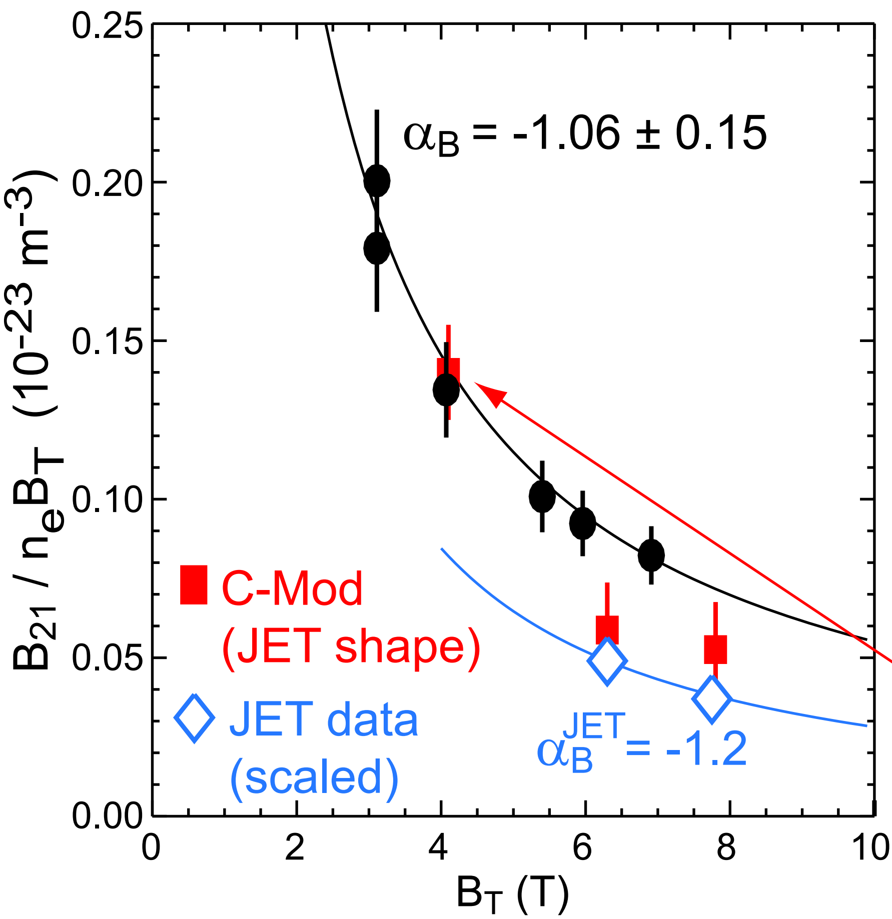

- Scaling of $\tilde{B} / B_T$ locking threshold is needed to extrapolate to ITER.

  $\alpha_n = 1$ (experiment)

  $\alpha_R = 2\alpha_n + 1.25\, \alpha_B$ (Connor-Taylor)

- C-Mod expt: B_T scan with $n \propto I_p \propto B_T$, $n/n_G = 0.17$, $q_{95} = 3.5$, $\tilde{B}_{11} / \tilde{B}_{21} = 1.4$.

- C-Mod data implies $\alpha_R = 0.68 \pm 0.19$ and projects to $\tilde{B}_{21}/B = 0.9 \times 10^{-4}$ at ITER's ohmic density (within ITER design constraint).

- JET/C-Mod identity experiments: JET shape, $\tilde{B}_{11} / \tilde{B}_{21} = 2.1$. Confirms Connor-Taylor & $\alpha_n = 1$.

- Caveat: Lower-field (4 Tesla) C-Mod locking threshold using the JET shape might imply a less favorable R scaling to ITER.

Scaling of intrinsic plasma rotation in H-mode from multiple tokamaks provides guidance for V_ϕ in ITER

$V_\phi \propto \Delta W/I_p$ in individual tokamaks, but size scaling is evident

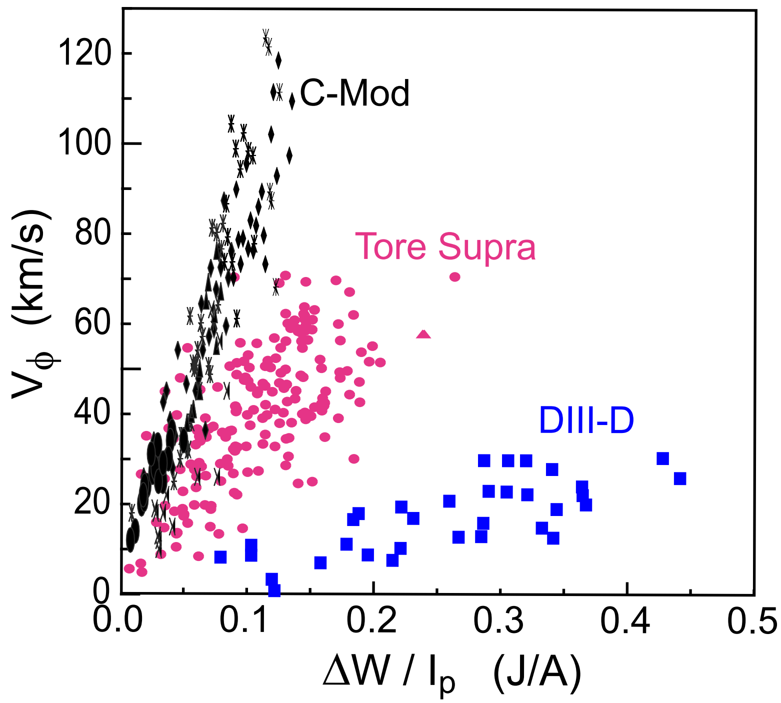

Results unified in plots of $M_i = V_\phi/C_s$ or $M_A = V_\phi/V_A$ versus β_N.

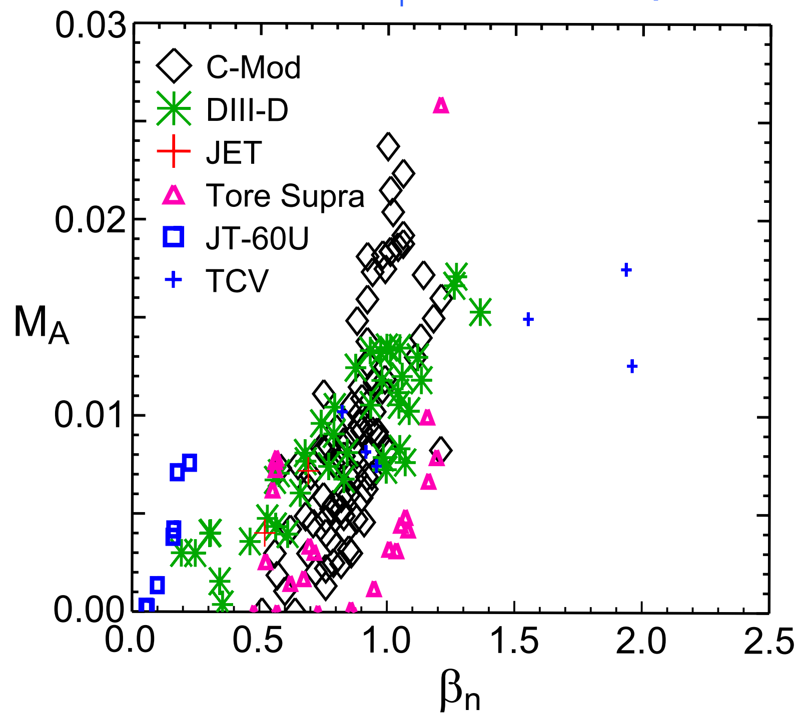

Parameter range		
a	0.21 - 1.2	m
R	0.67 - 3.4	m
B	1.4 - 5.4	Tesla
I_p	0.3 - 3.0	MA
W_p	0.04 - 4.0	MJ
V_ϕ	30 - 130	km/s

- No apparent correlation of V_ϕ or M with ν^* or ρ^*.
- Inferred scaling with β_N projects to $M_i = 0.3$ or $M_A = 0.02$ for ITER at β_N=2.6, V_ϕ= 250 km/sec, probably sufficient to stabilize RWMs.

Rice, EX/P3-12

Observation of TEM turbulence in tokamaks

Internal transport barrier (ITB) generated by off-axis RF heating, controlled with on-axis RF

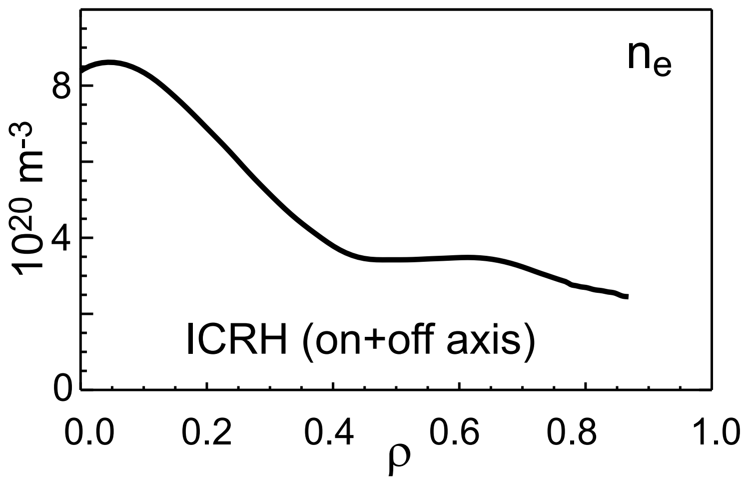

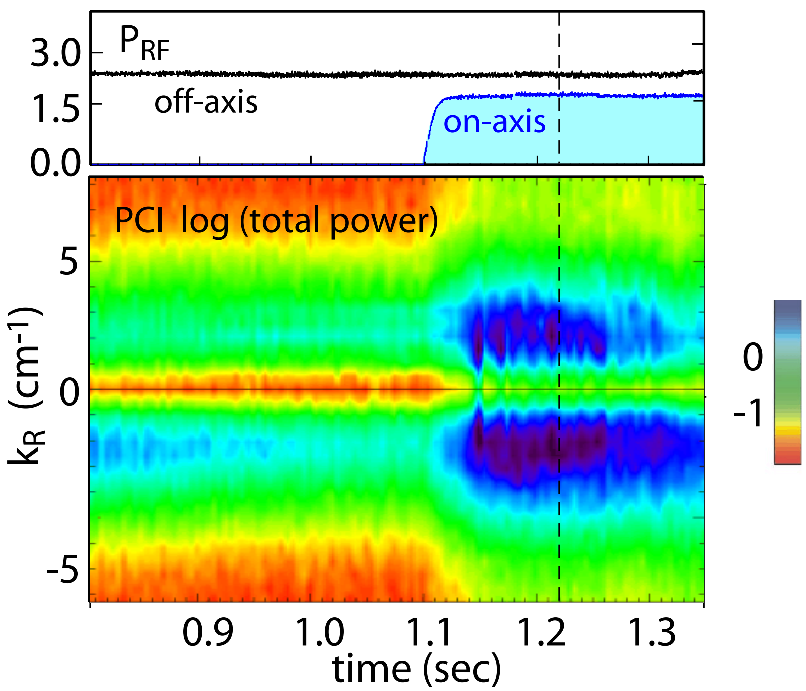

- On-axis heating increases $T_e \Rightarrow$ drives strong TEM in ITB. TEM limits electron density gradient and explains control of ITB with on-axis ICRH.

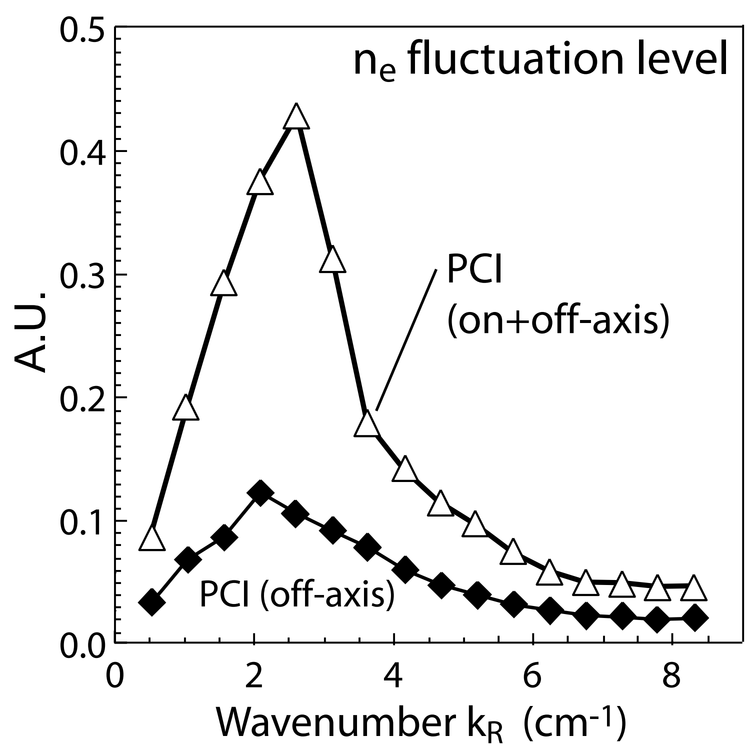

Ernst, TH/1-3

Observation of TEM turbulence in tokamaks

Alcator C-Mod

Internal transport barrier (ITB) generated by off-axis RF heating, controlled with on-axis RF

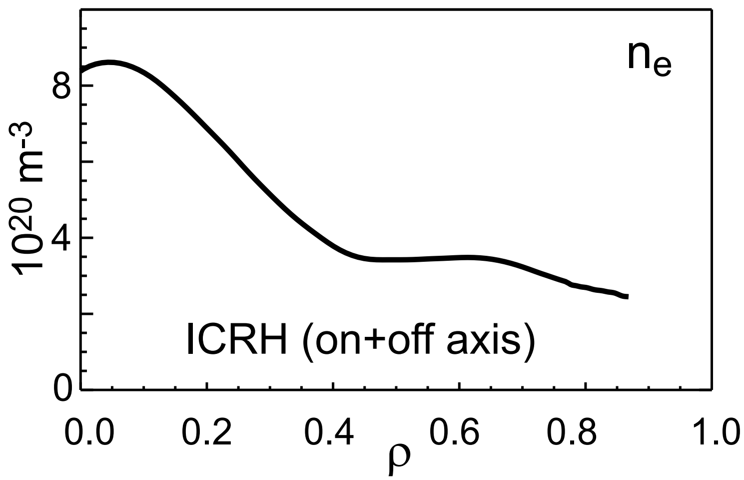

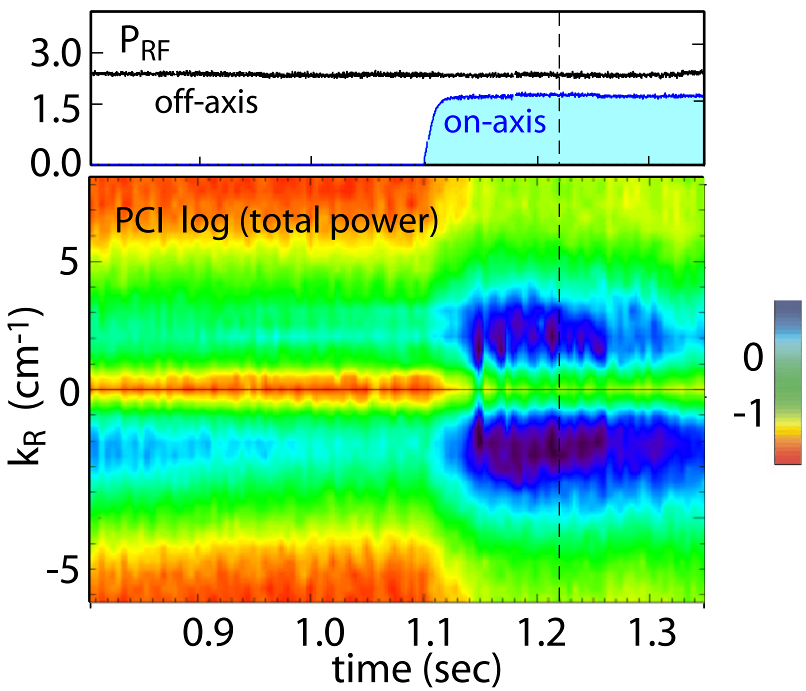

- On-axis heating increases $T_e \Rightarrow$ drives strong TEM in ITB. TEM limits electron density gradient and explains control of ITB with on-axis ICRH.
- Nonlinear GS2 gyrokinetic simulations with new synthetic PCI diagnostic reproduce:
  - wavenumber spectrum with on-axis ICRH.
  - increase in density fluctuation level with on-axis ICRH.

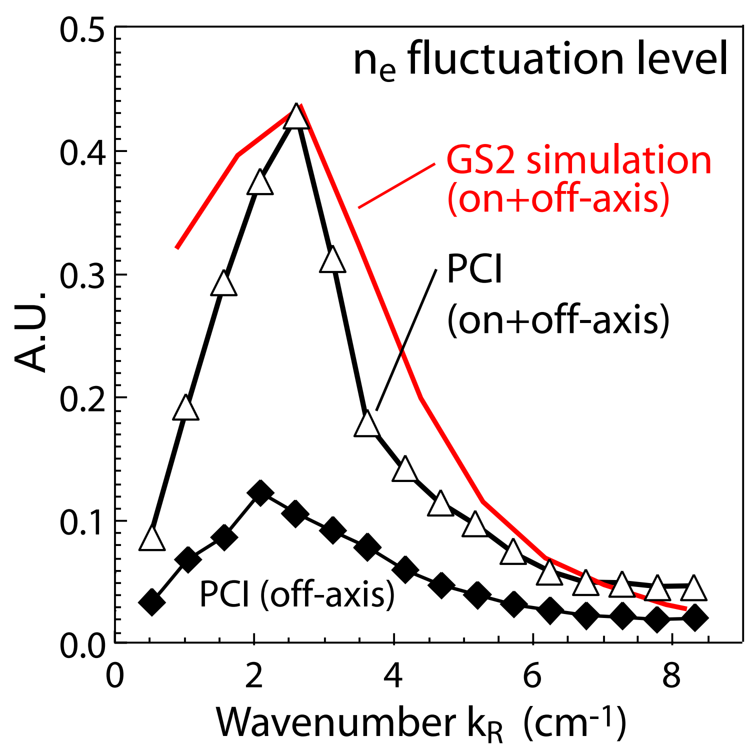

Ernst, TH/1-3

Nova-K with synthetic PCI diagnostic improves understanding of Alfven cascades

Alcator C-Mod

Phase Contrast Imaging (PCI) observes 'chirping' with multiple modes

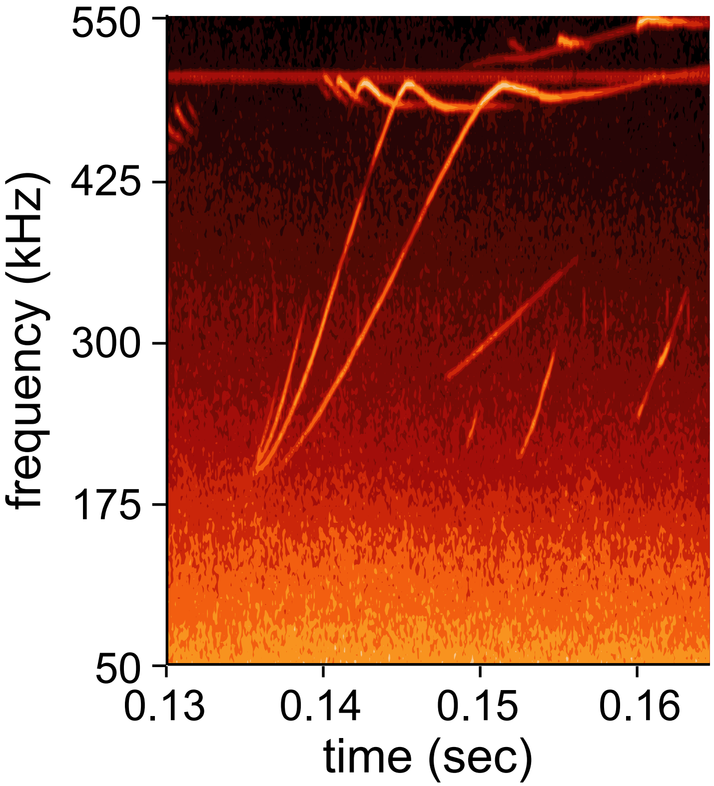

Alfven cascades produced by early ICRF when q(r) reversed, $q_{min} = 2$.

Nova-K with synthetic PCI diagnostic improves understanding of Alfven cascades

Alcator C-Mod

Nova-K calculations including GAMs reproduce measured frequencies

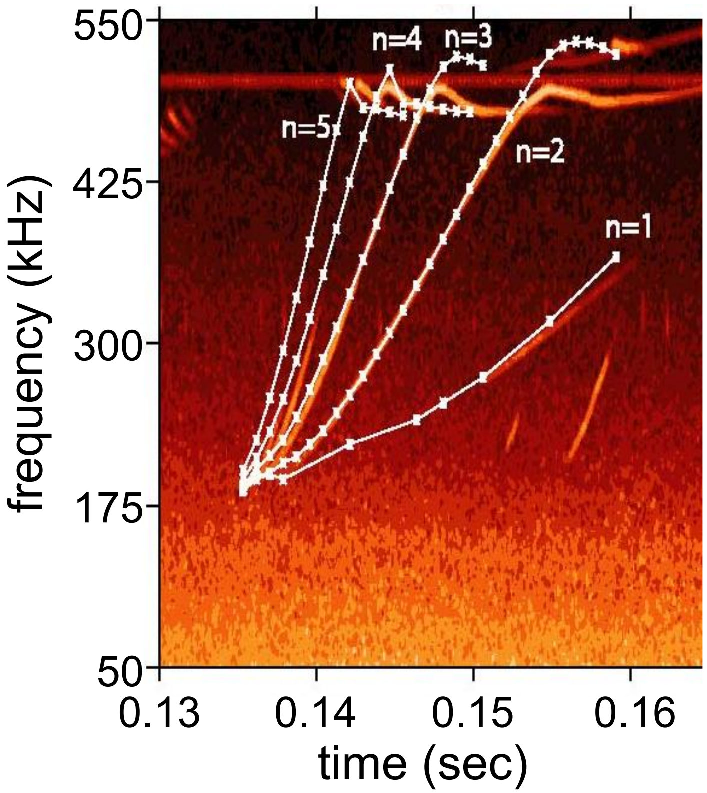

Chirping behavior is sensitive to q(r,t). Agreement with Nova-K indicates plasmas have RS.

Multiple peaks radially observed

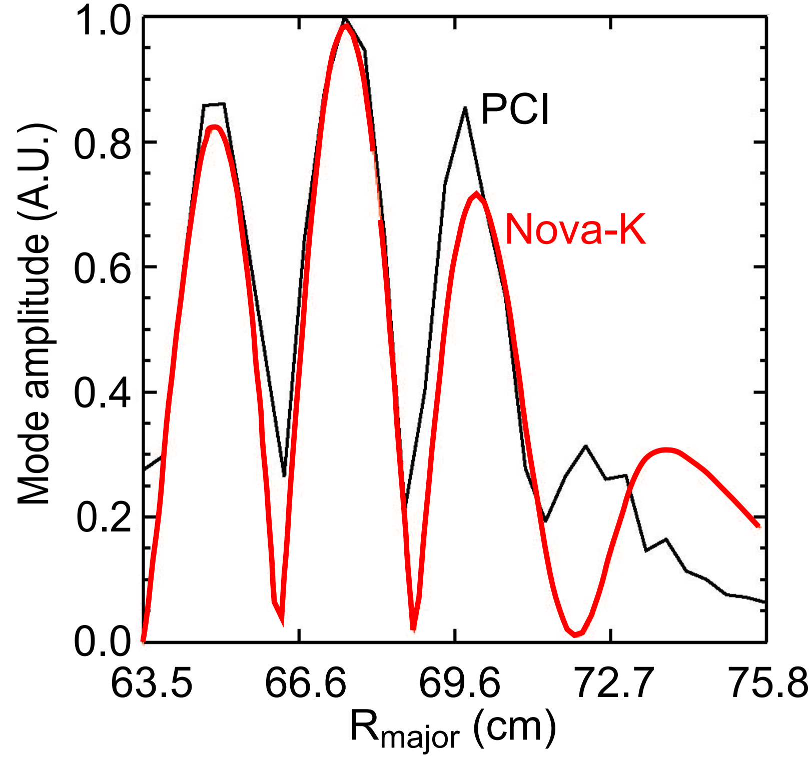

- Caused by multiple peaks in the actual radial mode structure, on artifact arising from integration along PCI sightlines?
- Synthetic PCI 'diagnostic' in NOVA-K indicates that multiple peaks consistent with a single radial mode.

Porkalab, EX/P6-16

Transport scaling near the separatrix is consistent with electromagnetic fluid drift 3-D Turbulence

Alcator C-Mod

- Theory: Turbulence & transport is controlled by two dimensionless parameters

  Beta Gradient: $\alpha_{MHD} \propto q^2 R \frac{\nabla_\perp P}{B^2}$ (inverse) Collisionality: $\alpha_d \propto \frac{1}{q}\left(\frac{\lambda_{ei}}{R}\right)^{1/2}\left(\frac{R}{L_n}\right)^{1/4}$

- Experiment: $\nabla P_e \propto I_p^2$ applies in both USN and LSN, but LSN achieves higher ∇P_e and higher α_{MHD}. Observed $\nabla P_e \propto I_p^2$ scaling consistent with EMFDT.

- Plasma flows are different in USN vs LSN, suggesting flows affect accessible values of α_{MHD}.

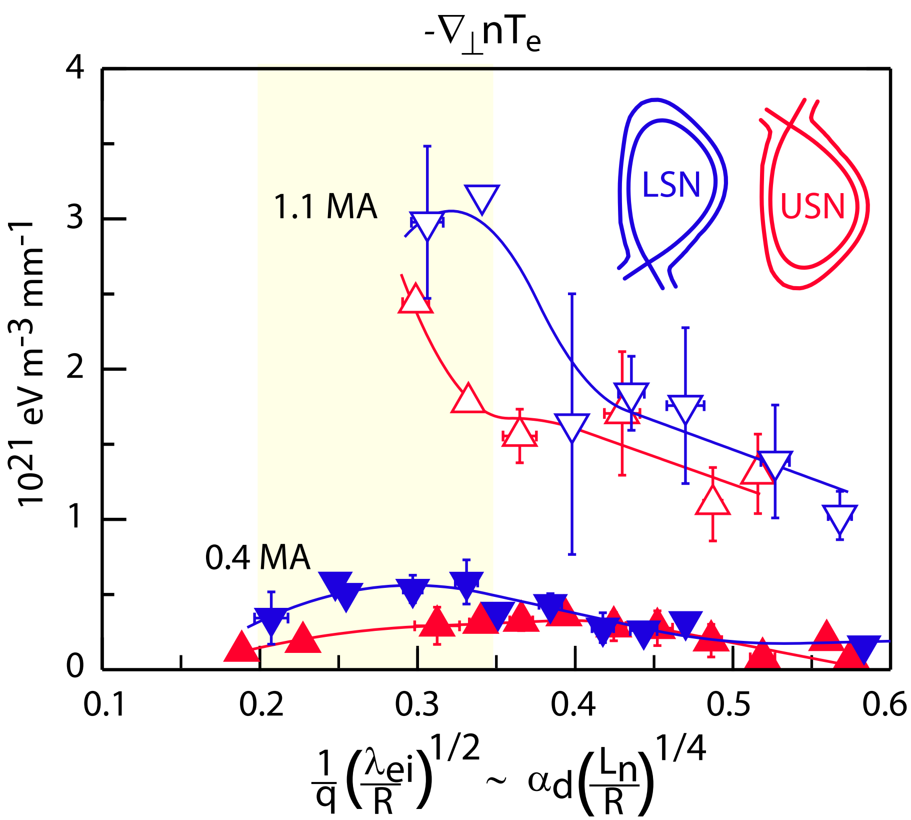

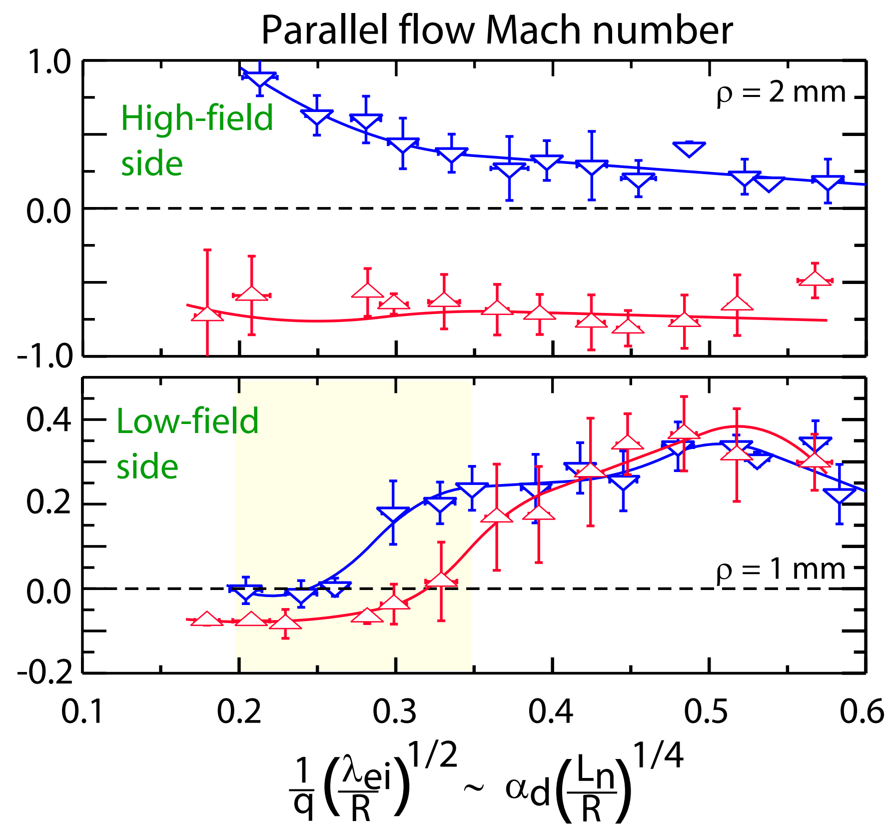

Intermittent turbulent structures ('blobs') at the edge have been measured with high temporal, 1-D and 2-D resolution

- SOL turbulence affects plasma-wall interaction, sets boundary condition for core plasma.
- Phenomonolgy important to guide & challenge first-principle models of intermittent transport in SOL.

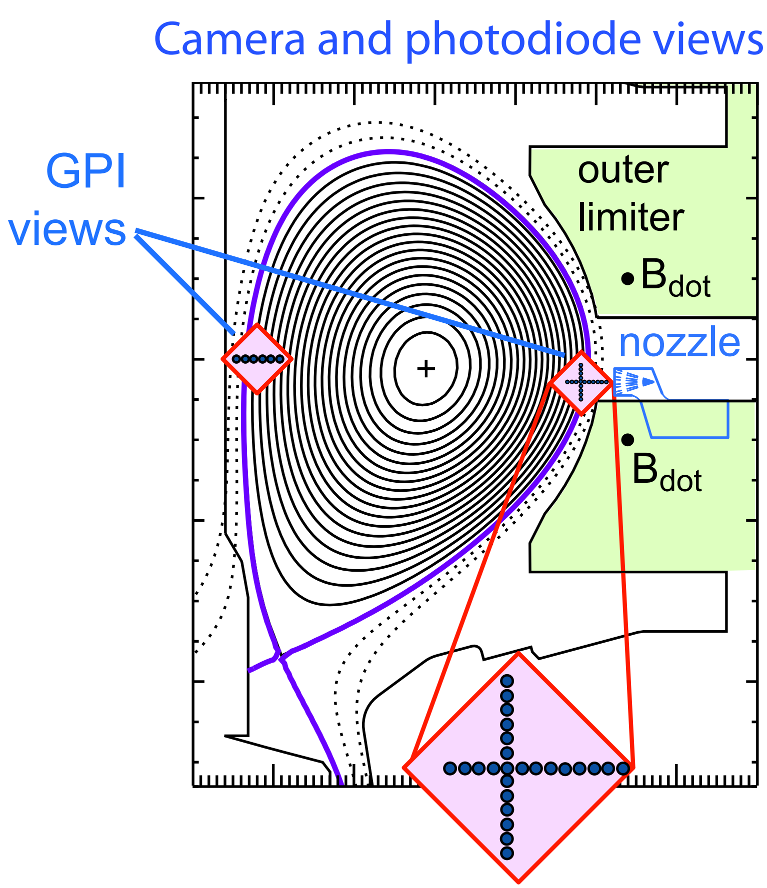

Intermittent turbulent structures ('blobs') at the edge have been measured with high temporal, 1-D and 2-D resolution

- SOL turbulence affects plasma-wall interaction, sets boundary condition for core plasma.
- Phenomonolgy important to guide & challenge first-principle models of intermittent transport in SOL.

Camera and photodiode views

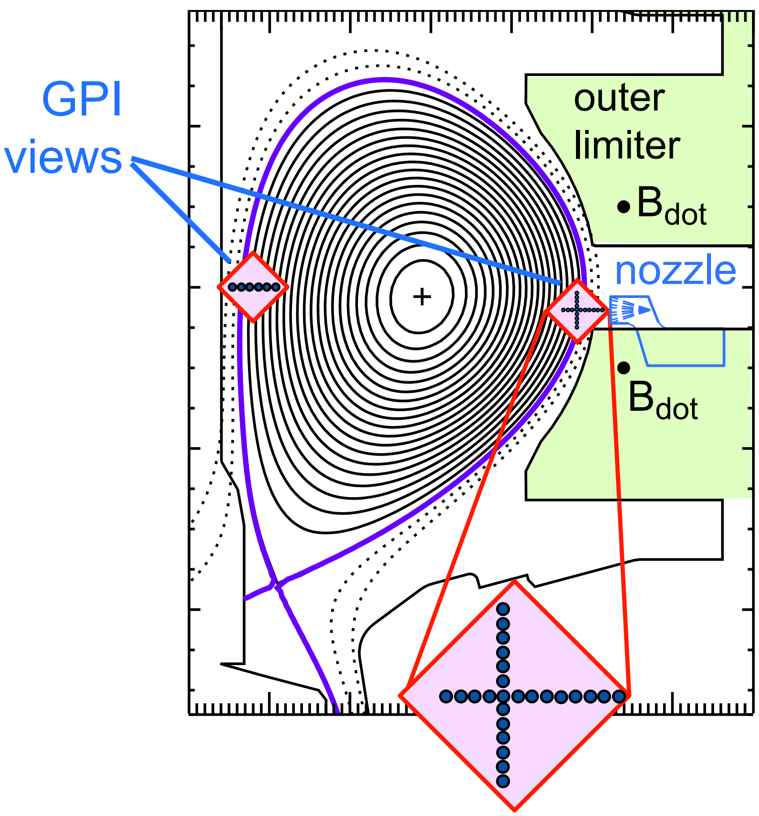

Blob flow patterns change across SOL into limiter shadow

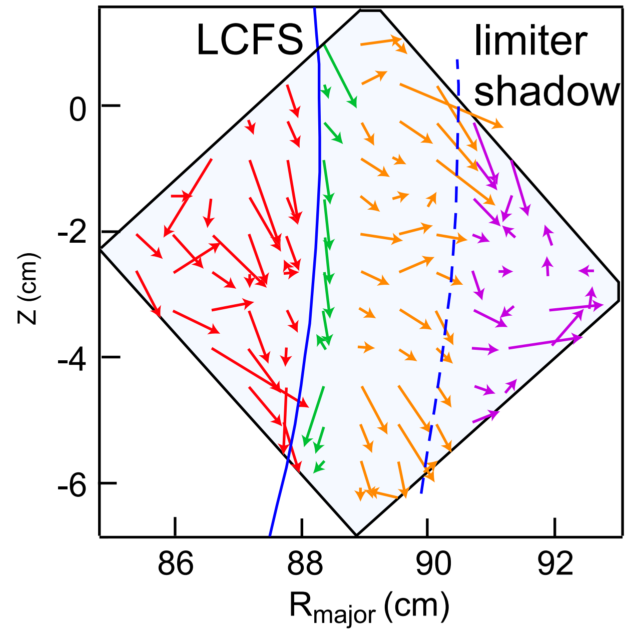

Blobs in the SOL have a net outward radial motion with a mean velocity ~1% of C_s

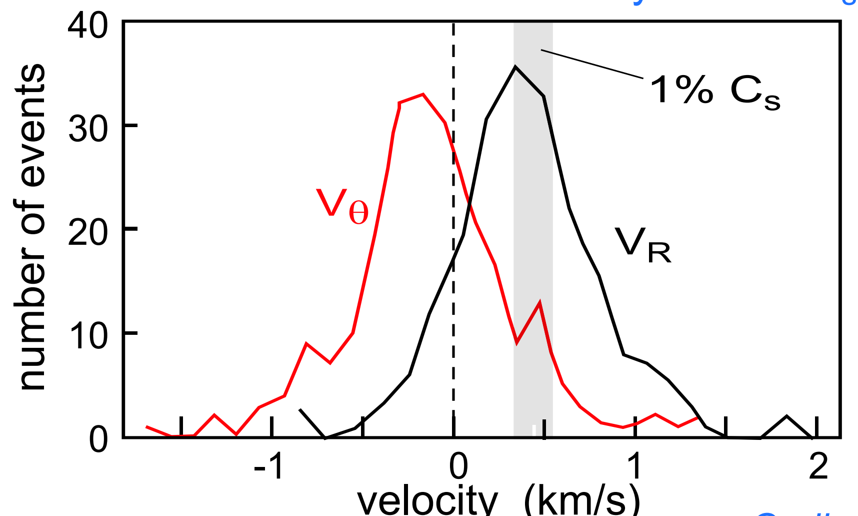

Grulke, EX/P4-7

Gas-puff imaging also used to study ELM dynamics at high resolution

- High triangularity, low ν* (<1) H-modes produce discrete ELMs with $\Delta W_{ped}/W_{ped}$ = 10-20% per ELM.

- ELM precursor: 200-400 kHz, $n_{toroidal}$ ~10 inside separatrix, propagates in ctr-I_p dir'n.

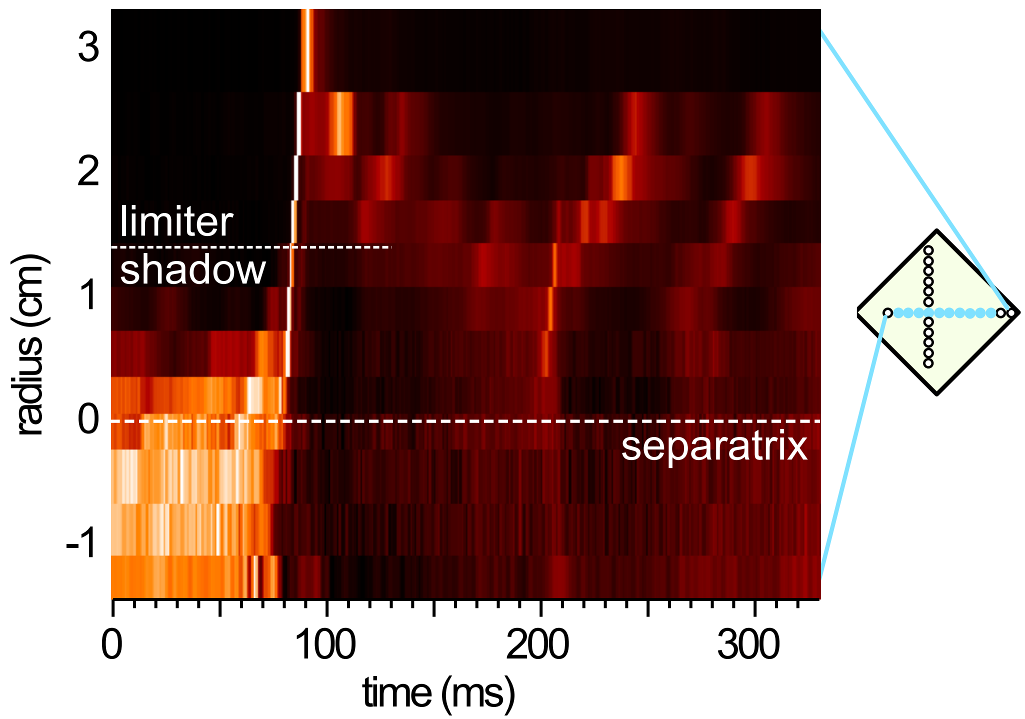

Gas-puff imaging also used to study ELM dynamics at high resolution

- High triangularity, low ν^* (<1) H-modes produce discrete ELMs with $\Delta W_{ped}/W_{ped}$ = 10-20% per ELM.

- ELM precursor: 200-400 kHz, $n_{toroidal}$ ~10 inside separatrix, propagates in ctr-I_p dir'n.

- Followed by ejection of rapidly propagating 'primary' filaments (V_R = 0.5 - 8.0 km/s), radial size 0.5 - 1.0 cm, at time of pedestal crash.

- 'Pedestal' on inboard and outboard sides is perturbed before ejection of filaments.

- 'Primary' is followed by multiple, slower secondary filament ejections.

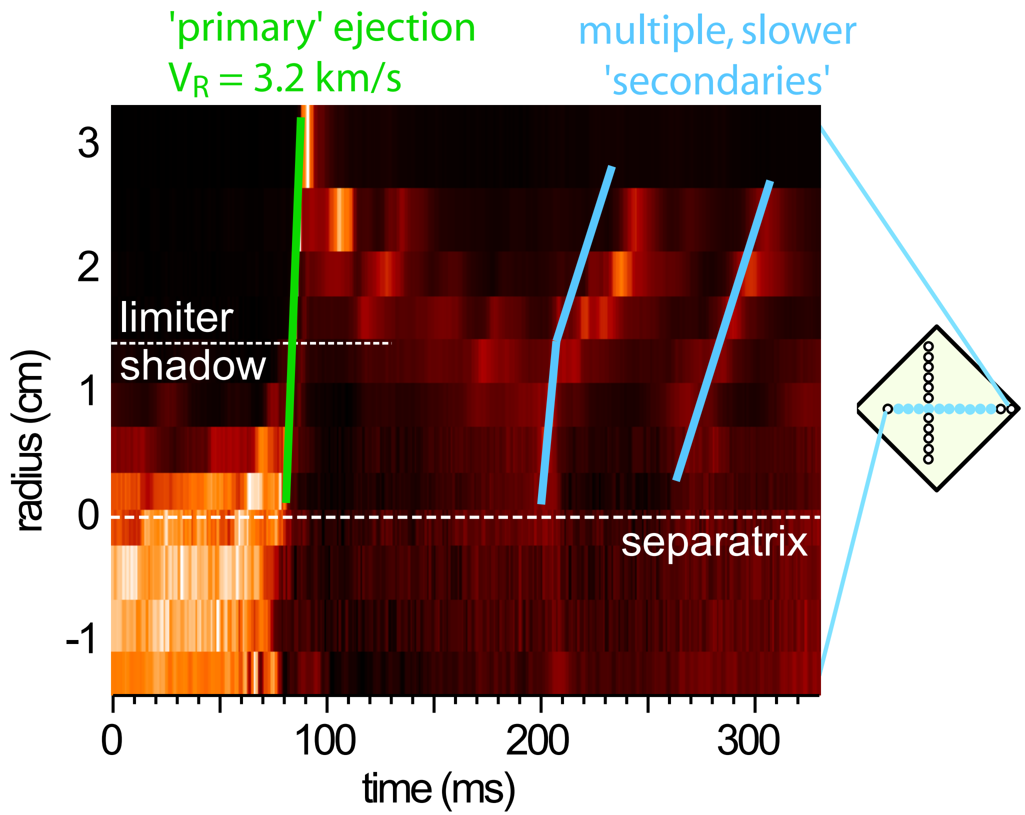

C-Mod Facility Upgrades 2006-8

toroidal cryopump

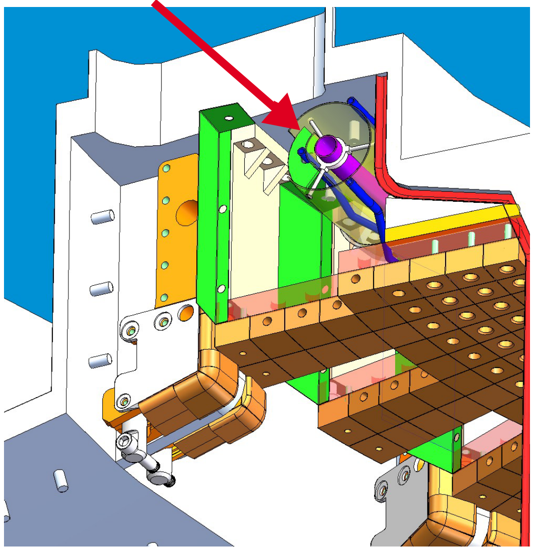

- Toroidal cryopump → density control in AT
- Tungsten belt in divertor → long pulse, high power
- 2nd LH launcher → 4 MW (source), compound spectra
- 2nd 4-Strap RF antenna → make room for LH
- Fast ferrite RF tuners → 1 ms response, tune thru ELMs
- Rotate DNB 7^{o} → resolve MSE calibration issues

tungsten belt lower divertor

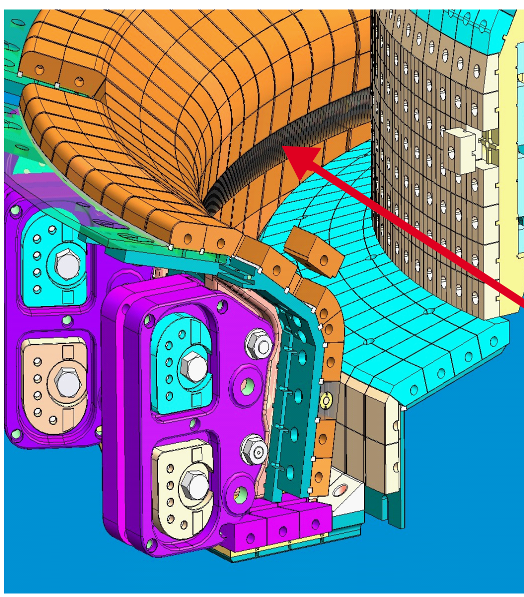

W lamellae tiles

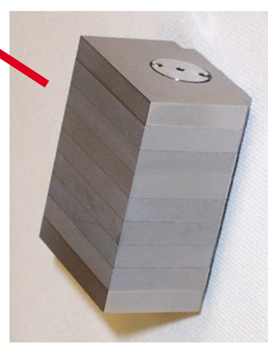

Summary

Alcator C-Mod

- Results favorable for ITER
  - disruption mitigation
  - LHCD
  - scaling of locked modes
  - scaling of intrinsic rotation
- Potential issues for ITER
  - plasma performance without low-Z PFCs or coatings
  - hydrogen retention in moly - worry for tungsten also?
  - erosion and impurity generation by RF sheaths
- Progress in physics basis for ITER
  - plasma edge understanding: SOL transport, 'blob' dynamics, ELM dynamics
  - Role of TEM in electron transport clarified
  - Alfven Cascade - radial structure